Regulation of *Caenorhabditis elegans* neuronal polarity by heterochronic genes

Maria Armakola and Gary Ruvkun

Gary Ruvkun
Email: ruvkun@molbio.mgh.harvard.edu

www.pnas.org/cgi/doi/10.1073/pnas.1820928116

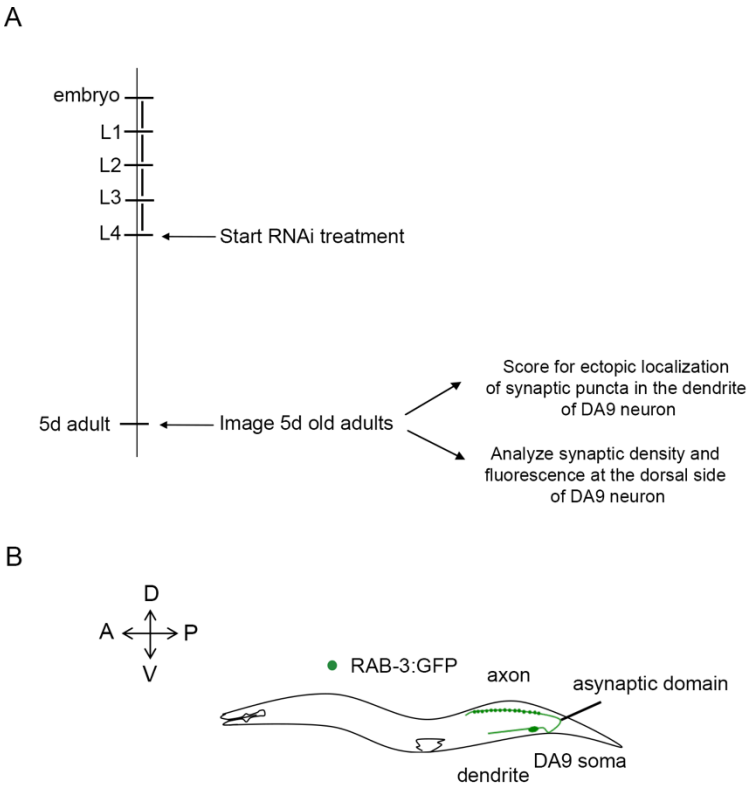

Fig.S1

Fig. S1. Experimental design used to identify gene inactivations that change RAB-3 localization in the DA9 neuron.

(*A*) Schematic of experimental timeline. Transgenic animals expressing GFP::RAB-3 in an RNAi hypersensitive background were fed with Ctrl RNAi or RNAi clones from a sublibrary of 135 RNAi clones that cause premature aging and scored for changes in localization of GFP::RAB-3 presynaptic marker when they were 5 days old. Animals were scored for ectopic dendritic localization of RAB-3 presynaptic marker at the ventral side and for changes in density and fluorescence of puncta at the dorsal side. Experiments were performed at 20ºC.

(*B*) Schematic diagram as seen from the left side of the worm. The DA9 cell body extends a dendrite anteriorly at the ventral side and an axon via a commissure at the

dorsal side where it forms *en passant* presynaptic terminals. Green dots represent GFP::RAB-3. A, anterior; P, posterior; D, dorsal; V, ventral.

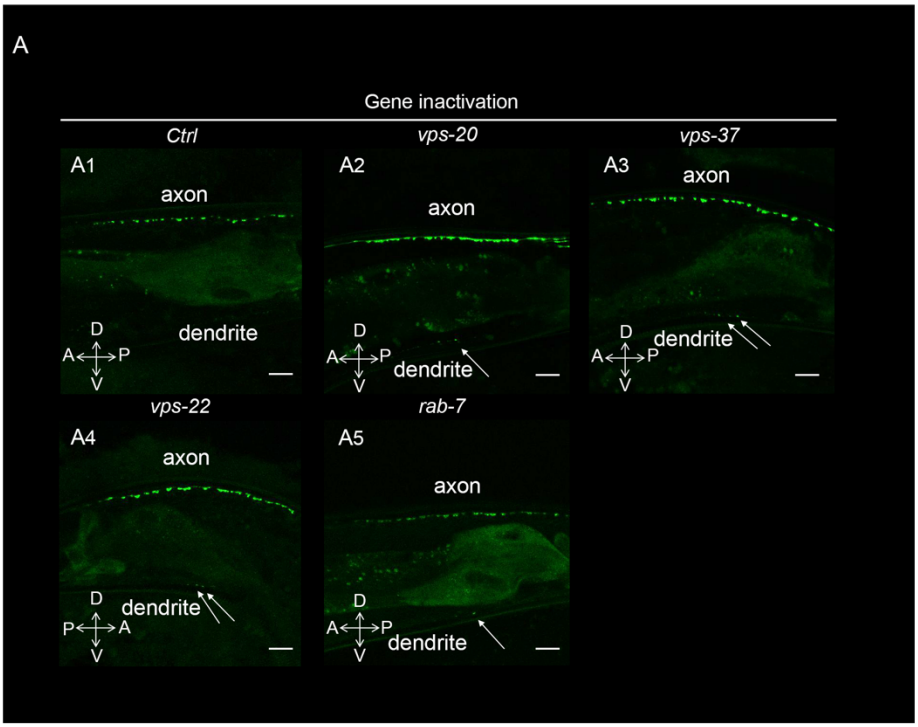

Fig.S2

Fig. S2. Gene inactivations of endosomal vesicular trafficking genes modify the localization of RAB-3 presynaptic marker in the DA9 neuron.

Among the hits from the screen were genes that regulate endosomal vesicular trafficking, such as *rab-7*, *vps-20*, *vps-22* and *vps-37*. (*A1-A5*) Representative linescans of *Pitr1::rab-3::gfp;nre-1(h20)lin-15b(hd126)* transgenic animals on different RNAi gene inactivations: empty vector (*ctrl*), *vps-20*, *vps-37*,*vps-22* and *rab-7*. Arrows indicate ectopic dendritic GFP::RAB-3 presynaptic puncta. A, anterior; P, posterior; D, dorsal; V, ventral. Images were taken at the 5-day old adult stage. Scale bars, 10μm.

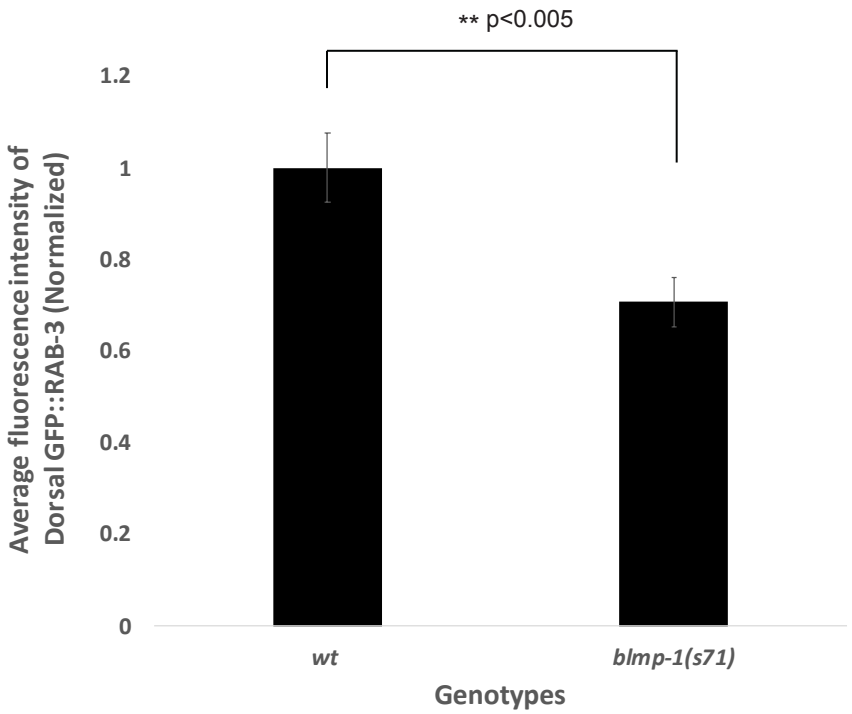

Fig.S3

Fig. S3. Dorsal presynapses have decreased fluorescence intensity in the dorsal side of *blmp-1(s71)* mutants compared to wt.

Quantification of average fluorescence intensity of dorsal GFP::RAB-3 at 5d old adult stage animals; n=45-47 worms in each genotype.**p<0.005, Student's t test. Error bars are SEM.

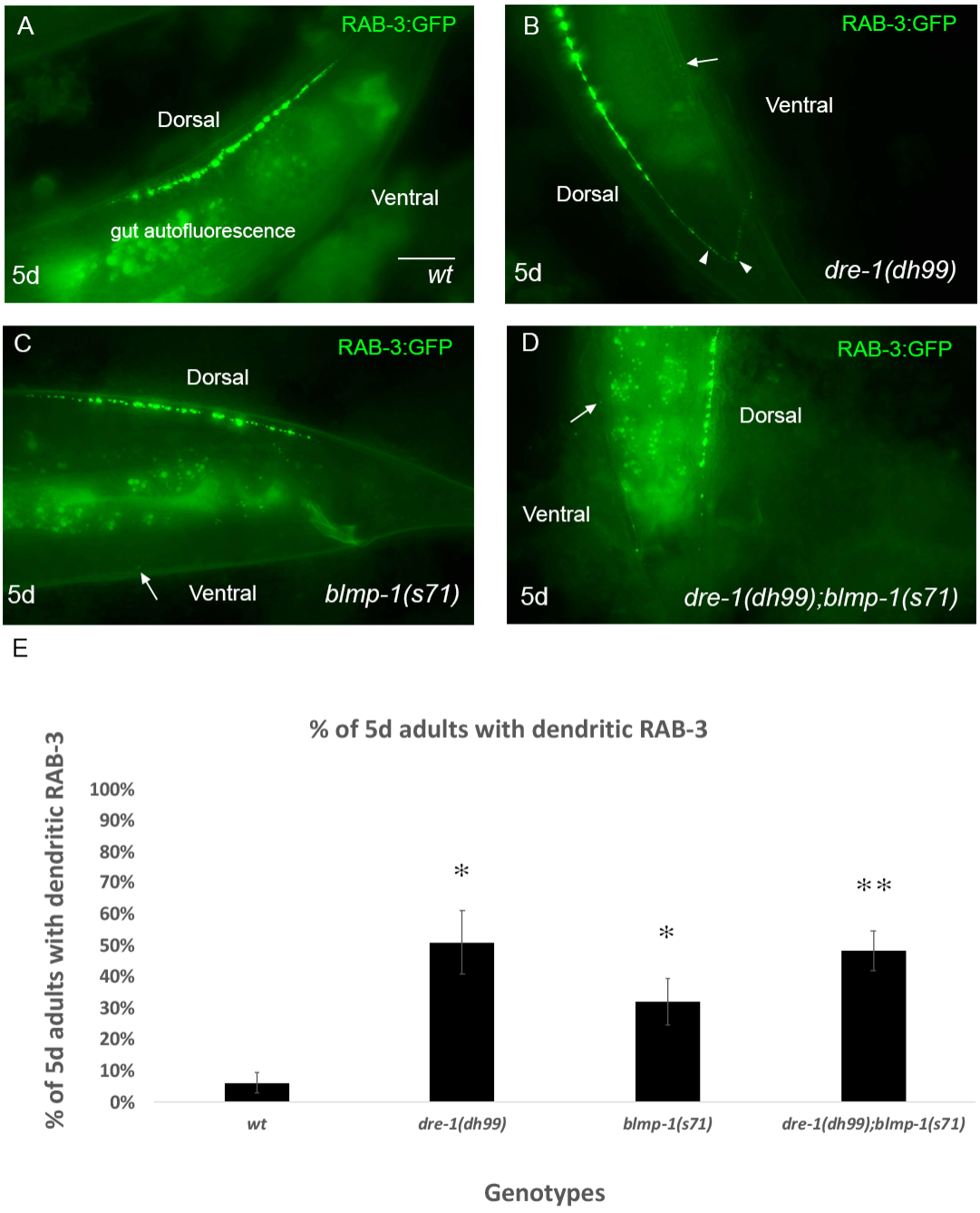

Fig.S4

Fig. S4. Testing the effect of RAB-3::GFP localization in *dre-1(dh99);blmp-1(s71)* double-mutant animals.

(*A-D*) *dre-1* acts in the same pathway as *blmp-1* to regulate synaptic polarity in DA9 neuron.

Representative images of animals expressing the presynaptic vesicle marker RAB-3::GFP in DA9 neuron in *wild-type* (A), *dre-1(dh99)* (B), *blmp-1(s71)* (C) and *dre-1(dh99);blmp-1(s71)* mutants (D). Animals were imaged when they were 5d old. Scale bar, 5μm. Arrows mark ectopic dendritic puncta. Arrowheads mark ectopic puncta at the asynaptic domain of DA9 neuron. The fluorescence in the middle of the worm is gut autofluorescence. Images were generated by an epifluorescence microscope. (*E*) Quantification of RAB-3::GFP puncta localization phenotype along the DA9. n=32-36 worms in each genotype. *$p<0.05$, **$p<0.005$ relative to wild-type, Student's t test. Error bars are SEM.

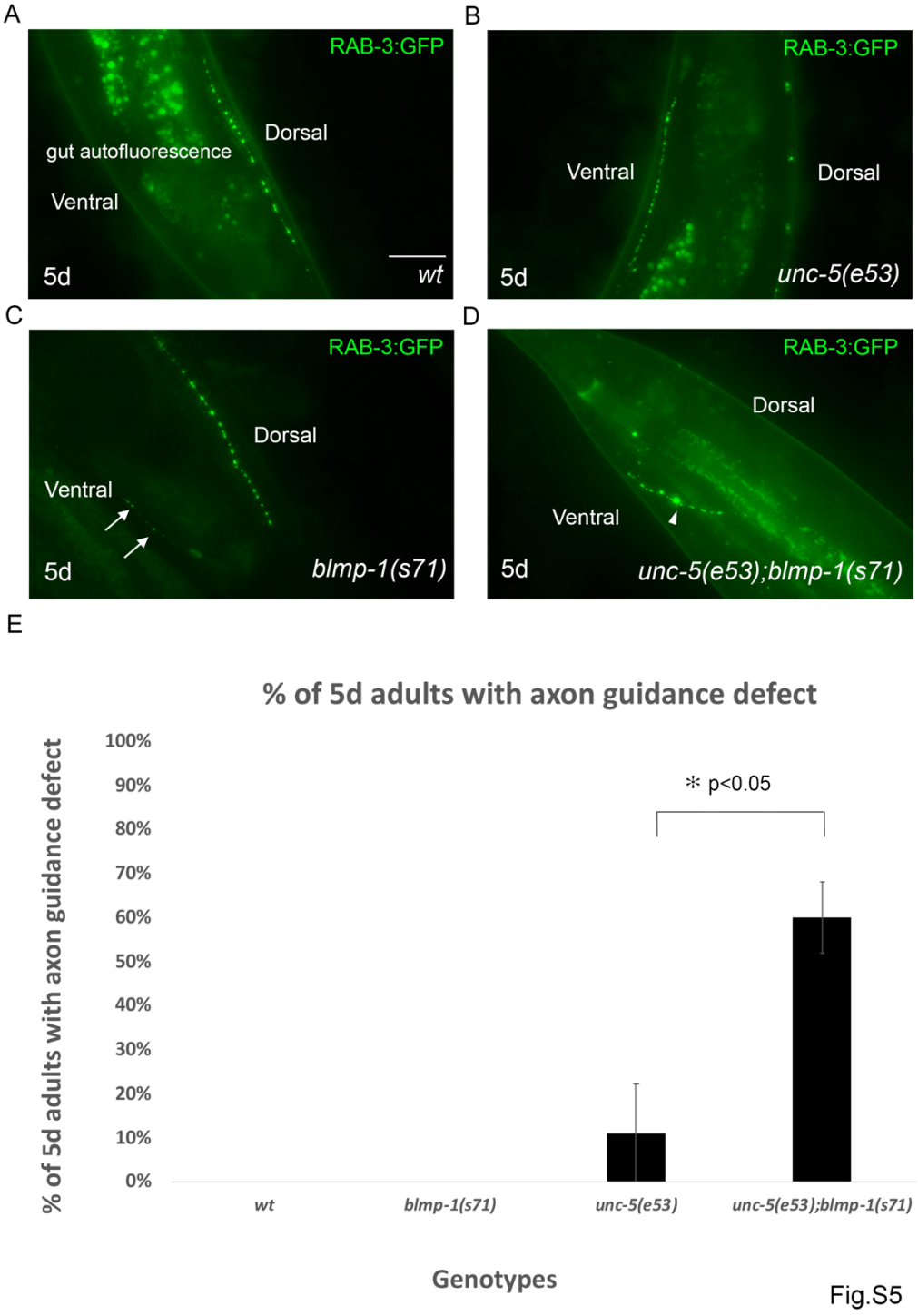
A
RAB-3:GFP
gut autofluorescence
Dorsal
Ventral
5d
wt
B
RAB-3:GFP
Ventral
Dorsal
5d
unc-5(e53)
C
RAB-3:GFP
Dorsal
Ventral
5d
blmp-1(s71)
D
RAB-3:GFP
Dorsal
Ventral
5d
unc-5(e53);blmp-1(s71)
E
% of 5d adults with axon guidance defect
% of 5d adults with axon guidance defect
100%
90%
80%
70%
60%
50%
40%
30%
20%
10%
0%
* p<0.05
wt
blmp-1(s71)
unc-5(e53)
unc-5(e53);blmp-1(s71)
Genotypes

Fig.S5

Fig. S5. Double-mutants *unc-5(e53);blmp-1(s71)* show an axon guidance defect and abnormal placement of RAB-3::GFP presynaptic puncta in DA9 neuron at 5d old adult stage.

(*A-D*) Loss of *blmp-1* function causes an axon guidance defect in DA9 neuron in *unc-5(e53)* mutant animals at 5d old adult stage. Whereas in *blmp-1(s71)* mutants RAB-3::GFP gets mislocalized in the dendrite at the ventral side, in the *unc-5(e53); blmp-1(s71)* mutants there is an axon guidance defect and abnormal placement of RAB-3::GFP presynaptic puncta in DA9 neuron. Representative images of RAB-3::GFP in *wild-type* (A), *unc-5(e53)* (B), *blmp-1(s71)* (C) and *unc-5(e53);blmp-1(s71)* (D) animals. Animals were imaged when they were 5 days old. Arrows mark the ectopic dendritic puncta observed in *blmp-1(s71)* mutant animals. Arrowhead indicates the abnormal axon guidance and placement of RAB-3::GFP presynaptic puncta in *unc-5(e53); blmp-1(s71)* mutants. Scale bar, 5μm. The signal in the middle of the worm is gut autofluorescence. Images were generated by an epifluorescence microscope. (*E*) Quantification of the abnormal axon guidance phenotype of the DA9 neuron at 5d old adults. n=26-30 worms in each genotype. *$p<0.05$, Student's t test. Error bars are SEM.

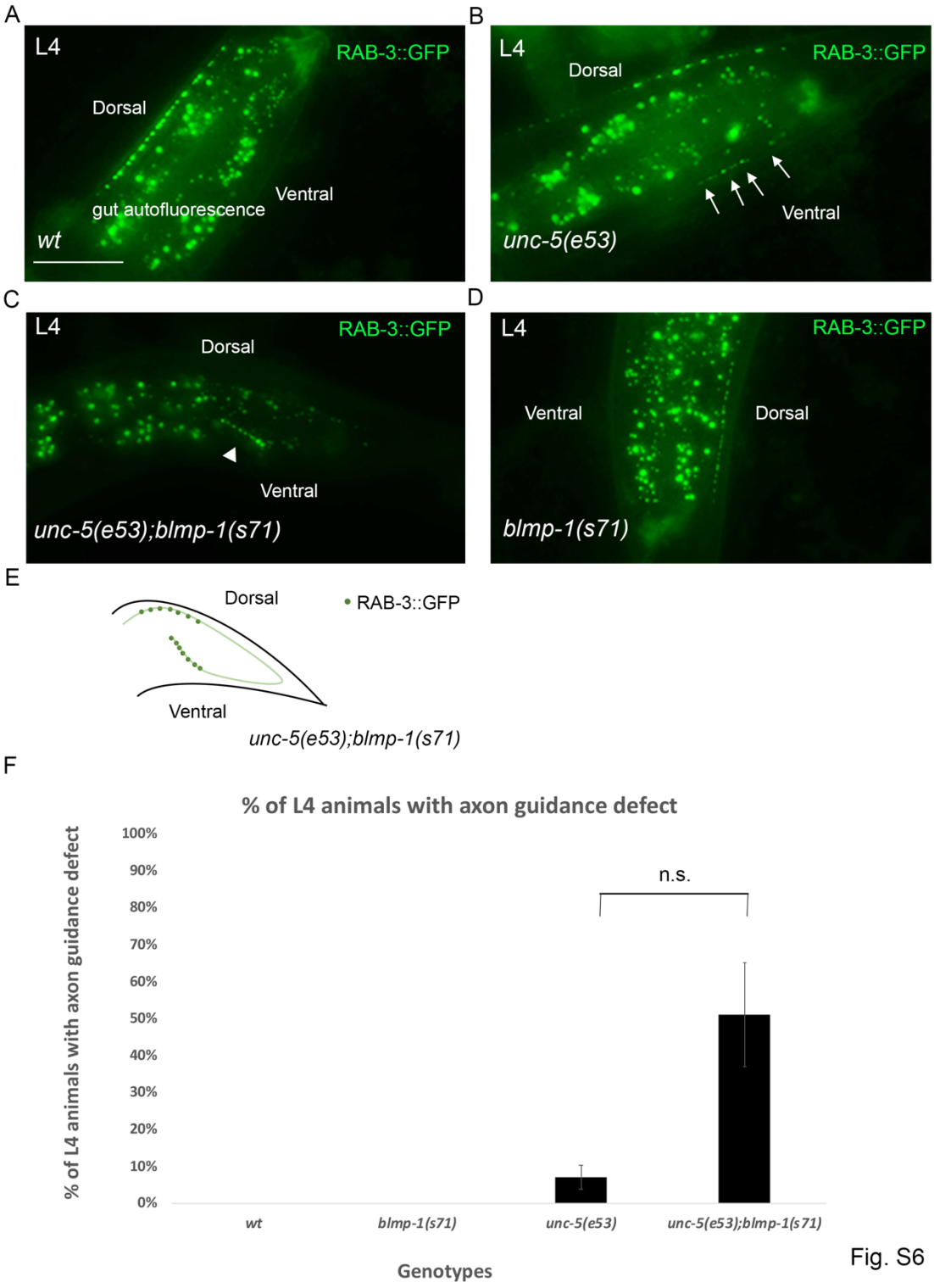

Fig. S6

Fig. S6. *unc-5(e53);blmp-1(s71)* double mutant animals show an axon guidance defect and abnormal placement of RAB-3::GFP presynaptic puncta in DA9 neuron at L4 developmental stage.

(*A-D*) Loss of *blmp-1* function causes an axon guidance defect in DA9 neuron in *unc-5(e53)* mutant animals at L4 stage. Whereas *blmp-1(s71)* mutants show no axon guidance defect, the *unc-5(e53); blmp-1(s71)* mutants show abnormal axon guidance and placement of presynapses at L4 stage. Representative images of RAB-3::GFP in *wild-type* (A), *unc-5(e53)* (B), *unc-5(e53);blmp-1(s71)* (C) and *blmp-1(s71)* (D) animals. Animals were imaged at L4 stage. Arrows mark the ectopic dendritic puncta observed in *unc-5(e53)* mutant animals. Arrowhead indicates the abnormal axon guidance and placement of RAB-3::GFP presynapses in *unc-5(e53); blmp-1(s71)* mutants. Scale bar, 5μm. The signal in the middle of the worm is gut autofluorescence. (*E*) A cartoon showing the abnormal placement of RAB-3::GFP presynapses observed in *unc-5(e53); blmp-1(s71)* mutants at L4 stage. Green dots represent RAB-3::GFP. Images were generated by an epifluorescence microscope. (*F*) Quantification of the axon guidance defect phenotype of the DA9 neuron at L4 stage. n=28-30 worms in each genotype. n.s. not significant, Student's t test. Error bars are SEM.

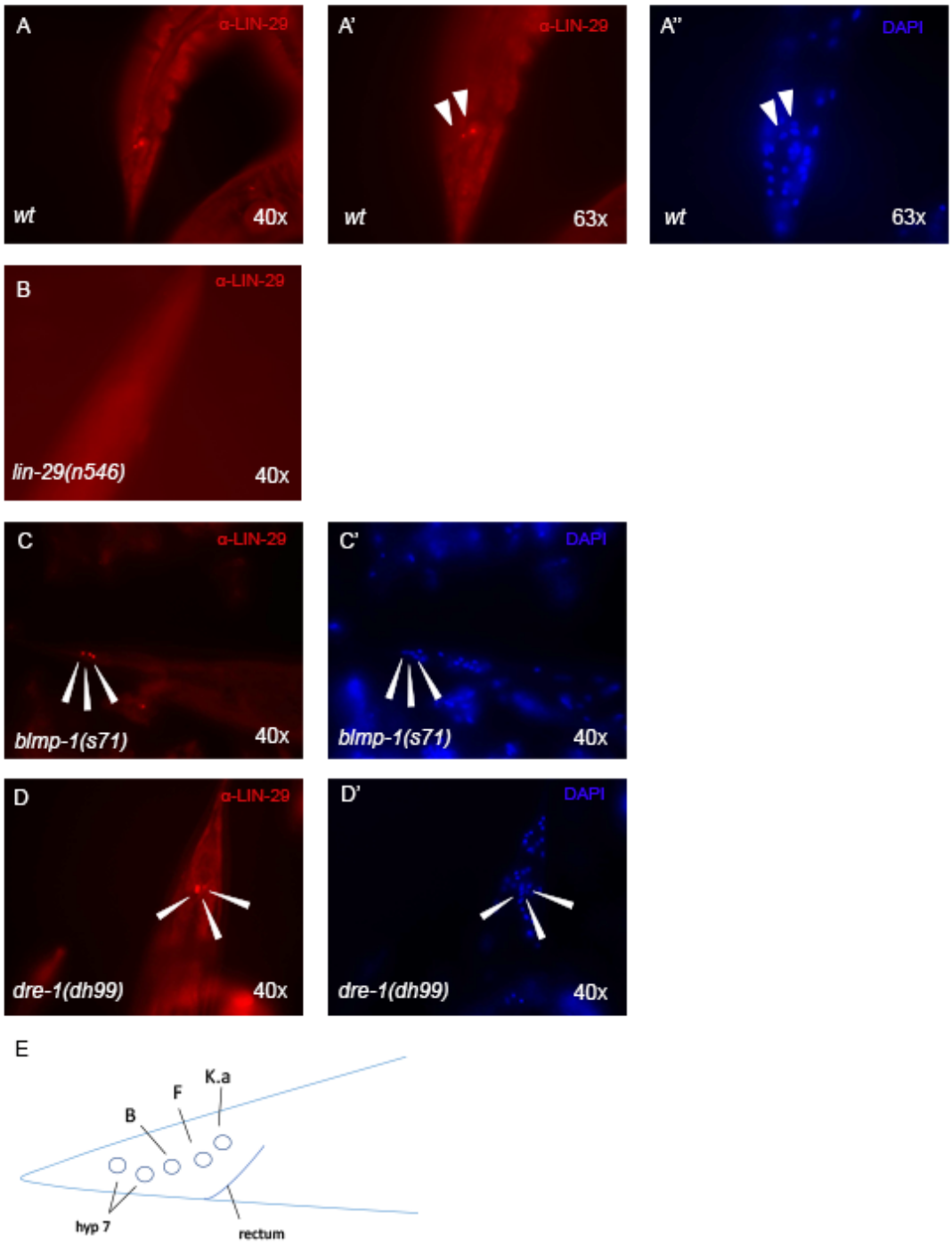

Fig.S7

Fig. S7. Effect of heterochronic mutations on LIN-29 protein immunofluorescence accumulation in non-hypodermal cells at the tail.

(*A*)-(*D*) Adult worms stained with α-LIN-29 antibody.

(*A*) Tail of a wild-type animal in adult stage stained with α-LIN-29 antibody and visualized by indirect immunofluorescence at 40x (*A*) and 63x (*A'*). (*A''*) DAPI staining of worm in (*A'*) to show nuclei. Arrowheads indicate the positions where LIN-29 is expressed at the tail of the worm.
(*B*) α-LIN-29 antibody staining in *lin-29(n546)* null mutant animals. In these mutants LIN-29 protein lacks the 86-amino acid C-terminal domain that is specifically recognized by the α-LIN-29 antibody. LIN-29 is not detected.
(*C*) α-LIN-29 antibody staining of a single *blmp-1(s71)* mutant in adult stage at 40x. (*C'*) DAPI staining of worm in (*C*) to show nuclei. Arrowheads indicate the positions where LIN-29 is expressed.
(*D*) *dre-1(dh99)* adult mutants stained with α -LIN-29 antibody magnified at 40x. (*D'*) DAPI staining of worm in (*D*) to show nuclei. Arrowheads indicate the positions where LIN-29 is expressed. LIN-29 is detected in two distinct bright foci.
(*E*) Schematic showing the rectal cells (B, F, K.a) and hypodermal nuclei where LIN-29 is expressed at the tail of the animal.

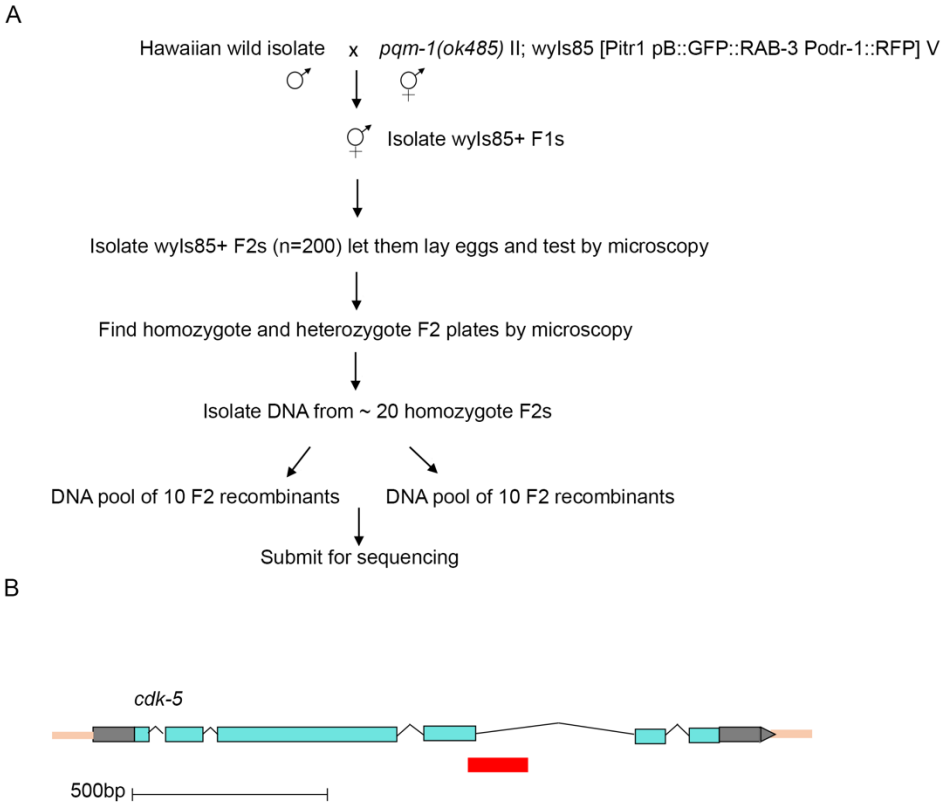

Fig.S8

Fig. S8. A deletion in *cdk-5* is the causative mutation for the mislocalization of RAB-3 presynaptic marker in the DA9 neuron.

(*A*) Schematic of outcross with Hawaiian strain.

(*B*) A cartoon showing the genomic region of III chromosome including the *cdk-5* gene. A 155bp deletion at Chr III (13,779,739-13,782,893) with an insertion of two bases (GA) starting from the last codon of exon 4 of *cdk-5* gene is indicated below the schematic of the genomic region.

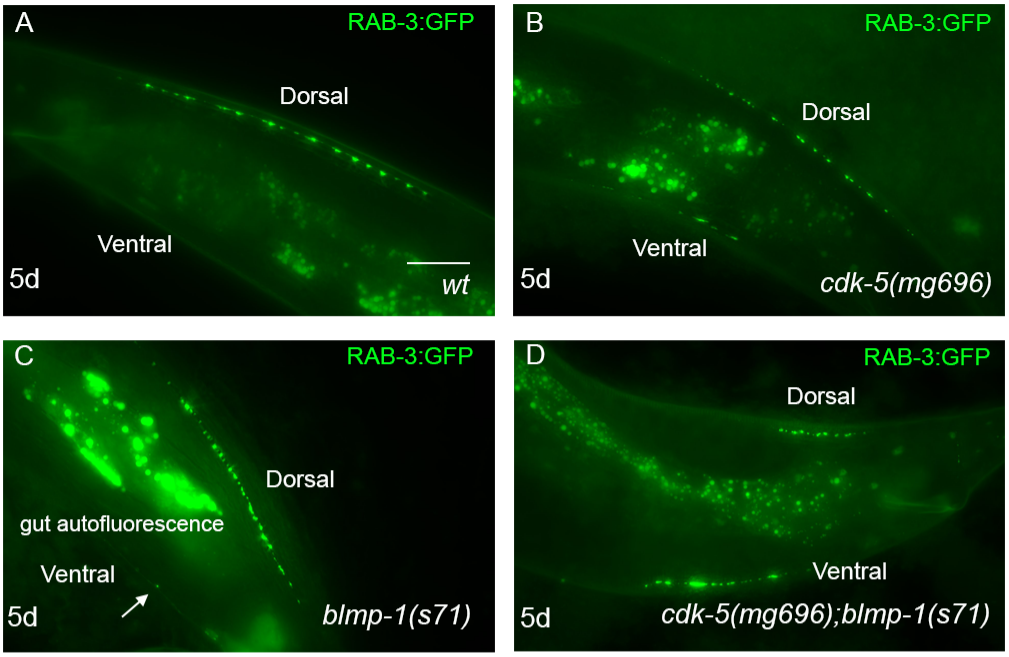
A
RAB-3:GFP
Dorsal
Ventral
5d
wt
B
RAB-3:GFP
Dorsal
Ventral
5d
cdk-5(mg696)
C
RAB-3:GFP
Dorsal
gut autofluorescence
Ventral
5d
blmp-1(s71)
D
RAB-3:GFP
Dorsal
Ventral
5d
cdk-5(mg696);blmp-1(s71)

E

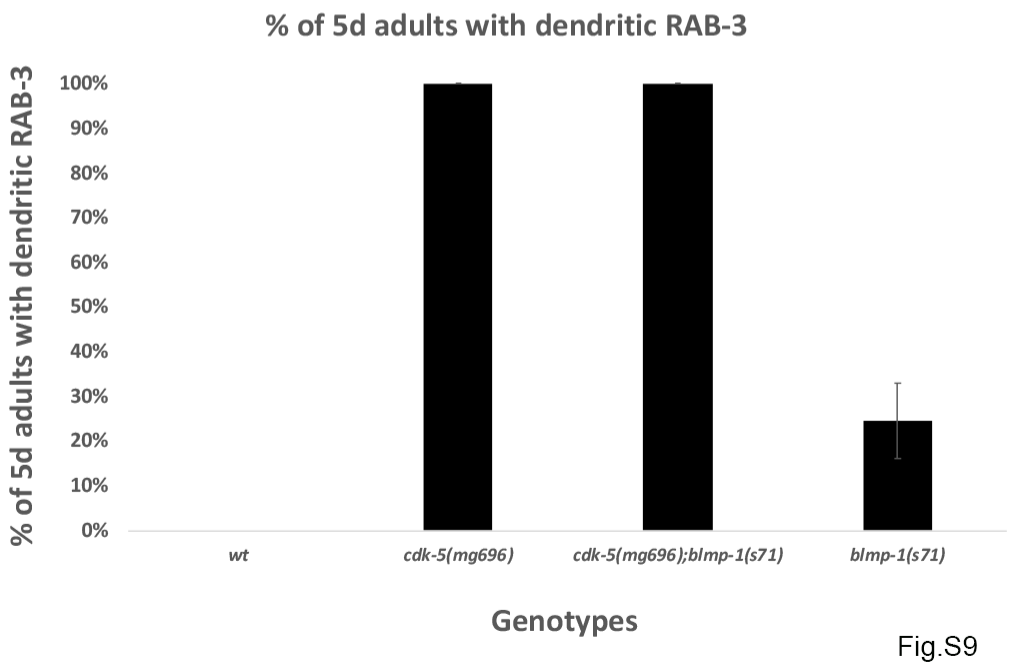
% of 5d adults with dendritic RAB-3
% of 5d adults with dendritic RAB-3
100%
90%
80%
70%
60%
50%
40%
30%
20%
10%
0%
wt
cdk-5(mg696)
cdk-5(mg696);blmp-1(s71)
blmp-1(s71)
Genotypes

Fig.S9

Fig. S9. RAB-3::GFP localization in *cdk-5(mg696);blmp-1(s71)* double mutant animals. (*A-D*) Loss of *blmp-1* function does not enhance or suppress the phenotype of *cdk-5(mg696)* mutants.

In both *cdk-5(mg696)* and *cdk-5(mg696); blmp-1(s71)* animals RAB-3::GFP is localized in both the dorsal and ventral sides of DA9 neuron.

Representative images of RAB-3::GFP in *wild*-type (A), *cdk-5(mg696)* (B), *blmp-1(s71)* (C) and *cdk-5(mg696);blmp-1(s71)* (D) mutant 5d old animals. Arrow marks the ectopic localization of RAB-3::GFP puncta at the ventral side in *blmp-1(s71)* mutant animals. Scale bar, 5µm. The fluorescence in the middle of the worm is gut autofluorescence. Images were generated by an epifluorescence microscope. (*E*) Quantification of ectopic dendritic RAB-3::GFP puncta phenotype. n=29-30 worms in each genotype. Error bars are SEM.

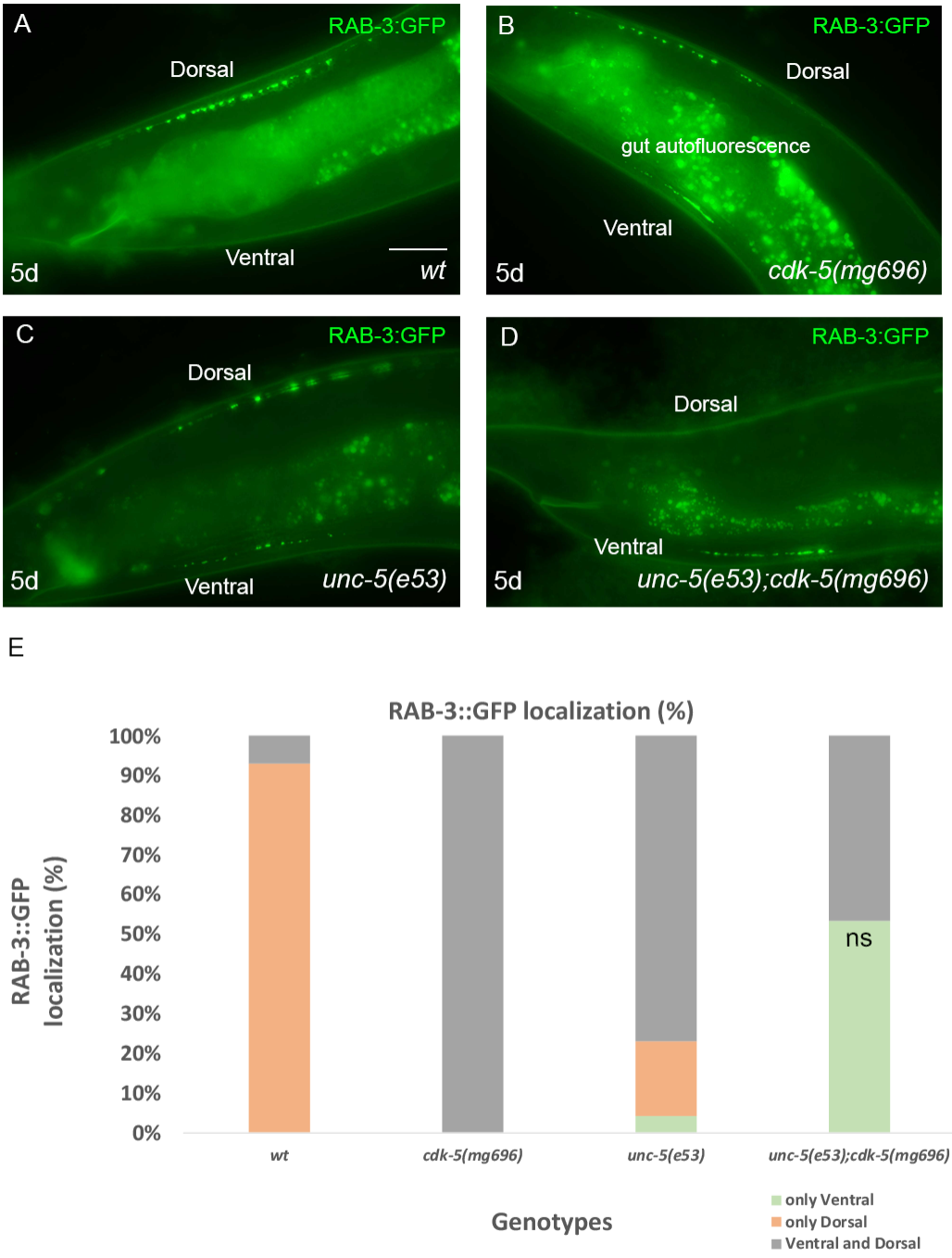

Fig.S10

Fig. S10. Loss of *unc-5* changes the localization of RAB-3::GFP puncta in *cdk-5(mg696)* mutants.

(*A-D*) *unc-5(e53); cdk-5(mg696)* mutants have less dorsal RAB-3::GFP signal compared to *cdk-5(mg696)* mutants alone. Whereas RAB-3::GFP is localized in both ventral and dorsal sides in *cdk-5(mg696)* and *unc-5(e53)* mutants, RAB-3::GFP signal decreases on the dorsal side and appears only at the ventral side in *unc-5(e53); cdk-5(mg696)* mutants. Representative images of RAB-3::GFP in *wild-type* (A), *cdk-5(mg696)* (B), *unc-5(e53)* (C) and *unc-5(e53);cdk-5(mg696)* (D) animals that are 5 days old. The transgene is *wyIs85*. Scale bar, 5μm. The fluorescence in the middle of the worm is gut autofluorescence. Images were generated by an epifluorescence microscope. (*E*) Quantification of the loss of dorsal RAB-3::GFP in *unc-5(e53);cdk-5(mg696)* mutants. The x axis indicates different genotypes tested. Green, orange and grey indicate worms showing RAB-3::GFP signal in "only Ventral", "only Dorsal", and "Ventral and Dorsal" sides, respectively. n=28-30 worms per genotype. ns, not significant relative to *unc-5(e53)*, Student's t test. Error bars are SEM. Symbol for statistics is labeled inside the green-filled bar for the phenotype of "only Ventral".

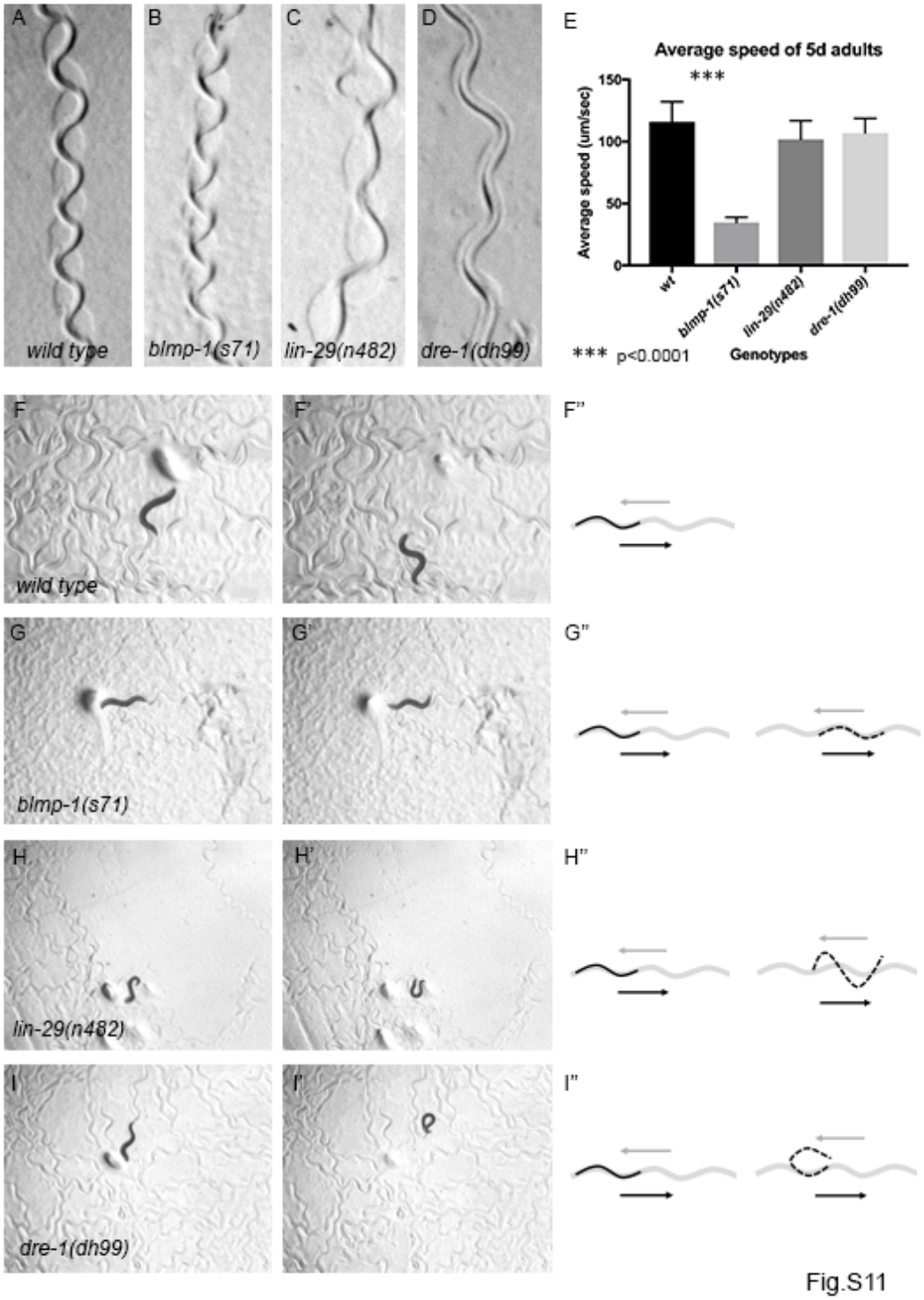

Fig S11. Backwards locomotion is altered in 5-day old heterochronic mutants.

(*A-D*) Images of tracks made by worms moving forwards. Wild-type (*A*), *blmp-1(s71)* (*B*), *lin-29(n482)* (*C*) and *dre-1(dh99)* (*D*).

(*E*) Quantification of the average speed of 5-day old heterochronic mutants after the tapping stimulus. *blmp-1(s71)* mutants display lower average speed comparing to wild type animals. Error bars indicate SEM. n=27-31 animals were analyzed per each genotype. (Mann-Whitney two-tailed t-test showed ***p <0.0001).

(*F-I*) Frames of movies of backward locomotion where the tapping stimulus is delivered at t=0 sec (*F-I*). (*F'*, *G*', *H'* and *I'*) are images of the final worm position t=10 sec after the tapping.

(*F''*, *G''*, *H''* and *I''*) are cartoons of typical backward locomotion stimulated by head touch for wild type (*F''*), *blmp-1(s71)* (*G''*), *lin-29(n482)* (*H''*) and *dre-1(dh99)* (*I''*) animals. Thick gray lines and gray arrows represent tracks and direction of forward movement. Solid black line represents the worm before the tapping stimulus. Dotted black line indicates the worm 10 sec after the tapping stimulus. Black arrow shows direction of backwards movement.

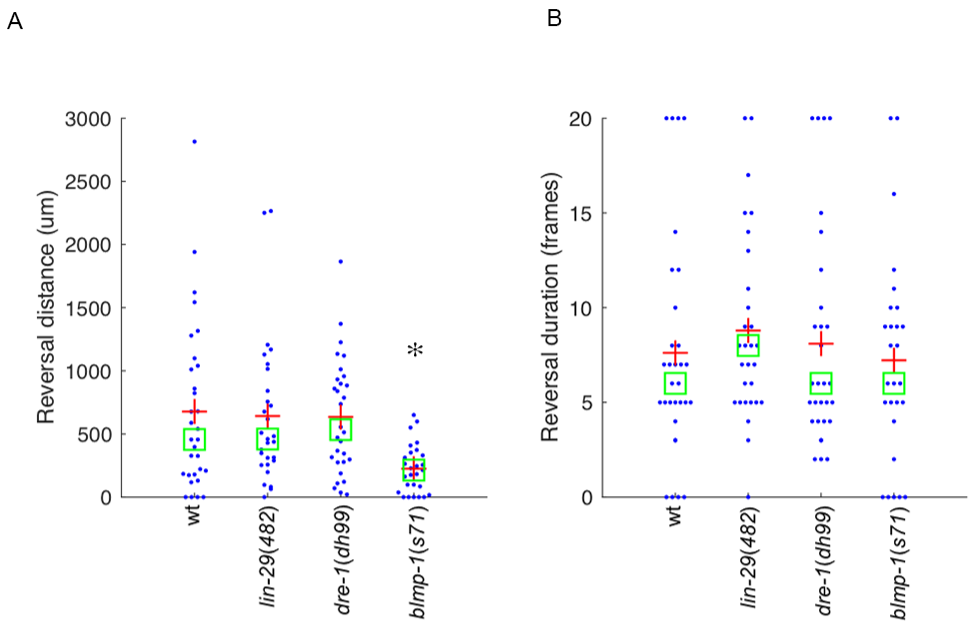

Fig.S12

Fig. S12. Quantitation of the reversal behavior of different heterochronic mutants.
(*A*) Quantification of the reversal distance measured in µm for *wt, lin-29(n482)*, *dre-1(dh99)* and *blmp-1(s71)* animals. Red crosses represent the mean value of reversal distance. Green boxes are centered on median values. *p<0.05 relative to *wt*, Anova with tukey post-hoc test.
(*B*) Quantification of the reversal duration calculated in frames (seconds) for *wt, lin-29(n482)*, *dre-1(dh99)* and *blmp-1(s71)*. Red crosses represent the mean value of the reversal duration. Green boxes are centered on median values.

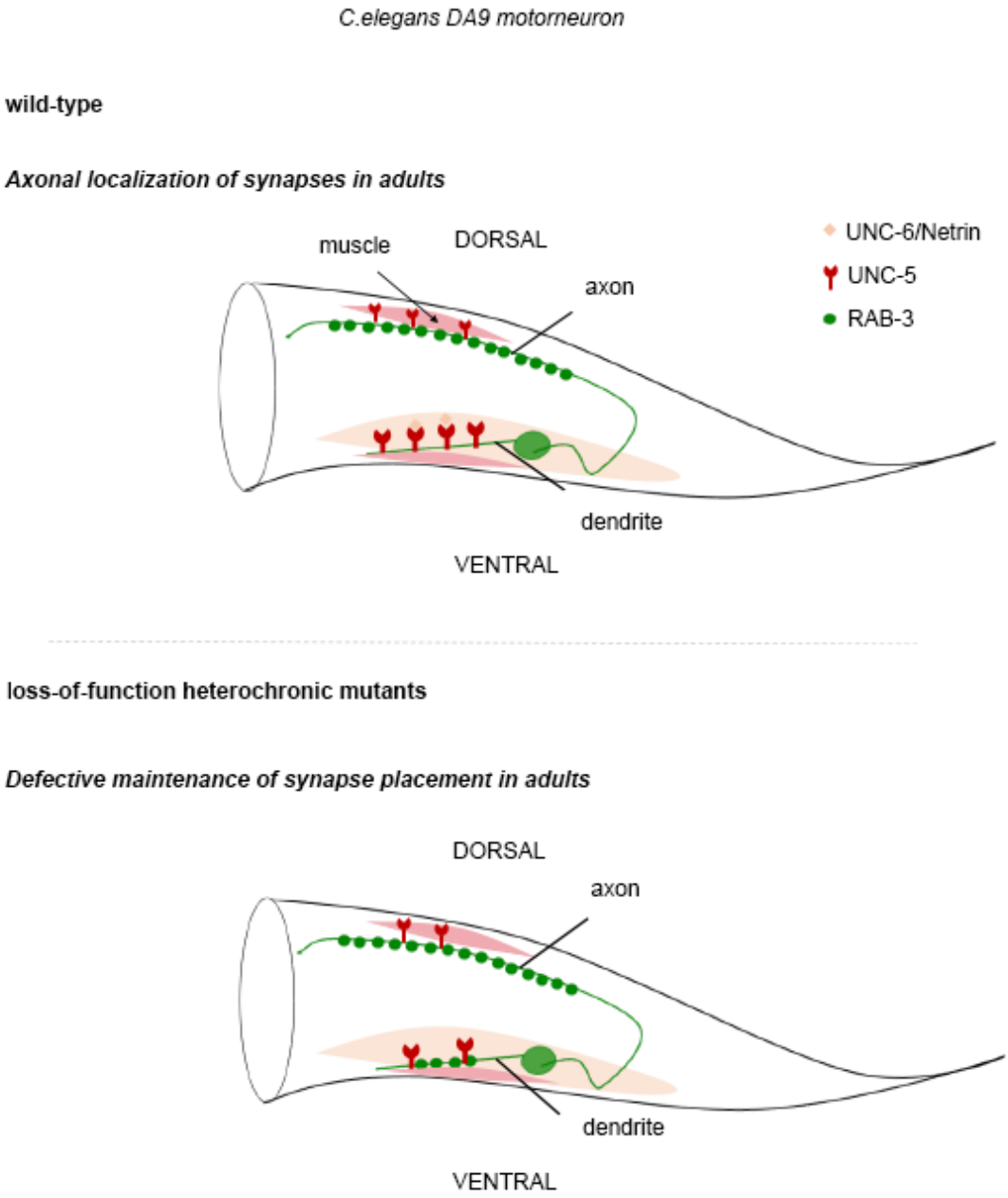

Fig. S13. Model for the action of heterochronic genes in the DA9 neuron.

In wild type animals UNC-6/Netrin guidance cues that are high ventrally and low dorsally bind to UNC-5 receptors in the dendrite to instruct axodendritic polarity in DA9. When heterochronic genes are mutant or inactivated the presynaptic marker RAB-3 is misplaced in the dendrites of the DA9 neuron, perhaps via regulation of UNC-5.

Table S1. Examples of gene inactivations that modify RAB-3 polarity in DA9 neuron

Gene inactivation	Molecular function	Class	Human ortholog	Ventral GFP::RAB-3 localization (%)	Change in intensity of Dorsal GFP::RAB-3[a] p<0.05	Change in density of Dorsal GFP::RAB-3[a]
Vector control	n/a	n/a	n/a	0%	n/a	n/a
sac-1	PIP phosphatase (yeast Suppressor of Actin) homolog	Protein trafficking	SACM1L	11%	yes	no
rab-7	Rab GTPases, vesicular trafficking	Vesicular trafficking	RAB7	15%	yes	no
C01F1.1	RAP74 (transcription initiation factor IIF)	Transcription	GTF2F1	30%	yes	yes
mvk-1	Mevalonate kinase, cholesterol biosynthesis	Signaling	MVK	22%	yes	no
vps-24	ESCRT-3 subunit, endosomal vesicular trafficking	Vesicular trafficking	CHMP3	29%	yes	no
vps-20	ESCRT-3 subunit, endosomal vesicular trafficking	Vesicular trafficking	CHMP6	36%	no	yes
vps-33.1	Vesicular docking and phusion	Vesicular trafficking	VPS33A	15%	yes	no
blmp-1	Transcription factor	Transcription	BLIMP1	22%	no	no
alg-2	PAZ and PIWI domain posttranscriptional gene silencing	Transcriptional regulation	AGO2	0%	yes	no
ptr-23	Intracellular cholesterol transport	Signaling	PTCHD3	0%	yes	yes
npp-3	Nucleoporin	RNA transport	NUP205	0%	yes	no
cua-1	ATP7A/MNK in late endosomes	Transport of small molecules	ATP7A	3%	yes	yes
C11H.3	Predicted E3 ubiquitin ligase	Proteolysis	MGRN1	7.5%	yes	yes
hda-1	Histone deacetylase 1	Transcriptional regulation	HDAC1	26%	no	no
cwc-15	Spliceosome-associated protein	Splicing	CWC15	30%	yes	no

[a] Relative to transgenic animals expressing RAB-3::GFP on control vector

Table S1. (continued)

Gene Inactivation	Molecular function	Class	Human ortholog	Ventral GFP::RAB-3 localization (%)	Change in intensity of Dorsal GFP::RAB-3[a] p<0.05	Change in density of Dorsal GFP::RAB-3[a]
gtf-2E1	General Transcription Factor homolog	Transcription	GTF2E1	35%	yes	no
F53H1.1	Helicase activity	Splicing	DDX46	37%	yes	no
tag-304	Protein binding	Signaling	GID8	26%	no	no
unc-23	Chaperone regulator	Cheperone regulation	BAG2	30%	no	no
T04G9.4	Magnesium ion binding activity	Metabolism	AASDHPPT	30%	no	no
dpy-3	Structural constituent of cuticle	Cuticle development	OTOL1	22%	no	no
vps-37	Related to yeast Vacuolar Protein Sorting factor	Vesicular trafficking	VPS37B/C	33%	no	no
calu-1	CALUmenin (calcium-binding protein) homolog	Calcium signaling	CALU	22%	no	no
cdgs-1	Phosphatidate cytidylyltransferase	Metabolism	CDS2	26%	no	no
inst-1	*INtegrator complex SubuniT 1 homolog*	Splicing	INTS1	22%	no	no
arx-4	Probable actin-related protein 2/3 complex subunit 2	Cell migration	ARPC2	27%	no	no
cbp-3	Histone acetyltransferase	Transcription regulation	EP300	30%	yes	no

[a] Relative to transgenic animals expressing RAB-3::GFP on control vector

Table S2. *C.elegans* strains used in this study

Strain	Genotype	Source
N2	wild type	CGC
	wyIs85 V or *Pitr1 pB::GFP::RAB-3 V*	K. Shen lab
	wyIs85 V; nre-1(hd20) lin-15b(hd126) X	cross
	blmp-1(s71) I; wyIs85 V	cross
	lin-29(n482) II; wyIs85 V	cross
	dre-1(dh99) V; wyIs85 V	CRISPR
	unc-5(e53) IV; wyIs85 V	cross
	lin-4(e912) II; wyIs85 V	cross
	lin-28(n719) I; wyIs85 V	cross
	wyIs85 V; lin-14(n179) X	cross
	wyIs85 V; daf-12(rh61) X	cross
	wyIs85 V; let-7(mg279) X	cross
	wyIs85 V; let-7(n2853ts) X	cross
	unc-29(kr208::tagRFP) I; wyIs85 V	cross
	unc-29(kr208::tagRFP) I; wyIs85 V; let-7(n2853ts) X	cross
	blmp-1(s71) I; dre-1(dh99) V; wyIs85 V	cross
	blmp-1(s71) I; unc-5(e53) IV; wyIs85 V	cross
	blmp-1(s71) I; *cdk-5(mg696) III; wyIs85 V*	cross
	cdk-5(mg696) III; unc-5(e53) IV; wyIs85 V	cross
	cdk-5(mg696) III; wyIs85 V	cross
RB711	*pqm-1(ok485) II*	CGC
CB4856	*C.elegans* wild isolate	CGC
VT516	*lin-29(n546)*/*mnC1*[*dpy-10(e128) unc-52(e444)*] II	CGC

Table S3. CRISPR guide RNA construct and repair template sequences

Plasmid (pJW1285 backbone)	**Guide sequence**	**Target**
pJW1285	gtgcatcatggttacactgg	*dre-1* exon 5
pNL243	GCTACCATAGGCACCACGAG	*dpy-10*
Repair oligo	**Sequence**	**Comment**
MA225	cgatgcgaagtgcatcatggttacactggaagtatctatgttcatgagagagga cgtggc	This is a repair oligo for the dre-1(dh99) substitution
MA262	AACTTCAATACGGCAAGATGAGAATGACTGGA AACCGTACCGCATGCGGTGCCTATGGTAGCGG AGCTTCACATGGCTTCAGACCAACAG	This is a co-conversion repair template for dpy-10(cn64)